Journal of Catalysis **181,** 145–154 (1999)
Article ID jcat.1998.2279, available online at http://www.idealibrary.com on IDEAL®

# Investigations of Palladium Catalysts on Different Carbon Supports

P. Albers,*[,1] R. Burmeister,* K. Seibold,* G. Prescher,* S. F. Parker,† and D. K. Ross††

*Degussa AG, P.O. Box 1345, D-63403 Hanau, Germany; †ISIS Facility, Rutherford Appleton Laboratory, Chilton, Didcot, OX11 0QX, United Kingdom; ††Department of Physics, University of Salford, Joule Laboratory, Salford M5 4WT, United Kingdom

Received July 6, 1998; revised August 14, 1998; accepted September 4, 1998

**Pd-catalysts (5 wt%) were prepared on various supports: powdered and pelletized activated carbon derived from pine wood or beech wood, carbon black, and graphitized carbon black. The supports were palladized in the original condition or after HCl-treatment. The catalysts were characterized with CO-chemisorption, transmission electron micrographs, and X-ray photoelectron spectrometry. The precious metal dispersion and the catalytic activity are improved by the acid treatment of activated carbon as well as carbon black supports. A selection of samples were also characterized by means of inelastic neutron scattering (INS) to study the hydrogen-related features of the acid modification of the carbon supports. Indications for different sensitivities of the final Pd/C-catalysts to catalytically driven hydrogasification effects of the supports and the impact of these effects on the precious metal dispersion and the formation of Pd-hydrides were obtained. The formation of molecular-like polyaromatic structures was observed especially on HCl-treated activated carbon due to enhanced spillover of active hydrogen from the Pd-particles to adjacent sites on the support. The generation and accessability of these sites on the support seems to be promoted by the removal of ash and adsorbed species.** © 1999 **Academic Press**

## INTRODUCTION

Activated carbons are widely used for the preparation of powdered and fixed-bed catalysts on a technical scale (1–4). These materials with very large surface areas (up to 1500 $m^2/g$) are derived from natural resources such as beech, oak, or pine woods, coconut shell, peat, lignite, or anthracite. In the catalyst manufacture, interactions between precious metal solutions and carbon supports are predominantly governed by chemical reactions at active surface groups (1–4) and/or adsorption sites with locally enhanced electron density or redox activity (5–11). The purity of the support, the ash content, the nature, and the concentration of surface groups and of active sites (6), the C/H-ratio, the microstructure characterized according to porosity and pore size distribution, all depend on the activation procedures of activated carbons. A great variety of activated carbons with different degrees of aromatization/graphitization are used for supported catalysts and it is widely accepted that catalyst efficiency is largely determined by the microstructure of the support and its surface properties (6–11). Related observations on carbon blacks as catalyst supports led to similar conclusions (12).

In addition to the properties of the carbon catalyst supports, the choice of the precious metal salts or precursors which are most suitable for the given catalyst application has a significant effect on the activity and selectivity of the final catalysts (13).

Acid treatments of the carbon supports reduce the ash content and the impurity level. Furthermore, controlled oxidative modifications of the surface can be obtained by means of $HNO_3$, NaOCl, $H_2O_2$, etc. These treatments could favour dispersion of the metal, with adequate mean-valence, in the final supported catalyst (14, 15).

Secondary ion mass spectrometry (SIMS) measurements have revealed a significant impact of acid treatments on the C/H-fragmentation characteristics, e.g. on the relative intensities of the $CH^-$, $C_2^-$, $C_2H^-$, and $C_2H_2^-$ entities. They reflect changes in the surface ratio of C/H-structures of lower and of higher crystallinity, as a consequence of the cleaning pretreatment of the catalyst support (15). Distinct changes of the fragmentation patterns of carbons were also observed after oxidizing treatments (16).

With references to the hydrogen-related properties of carbon supports, it was suspected that, in addition to chemically active hydrogen from OH-groups in the support, hydrogen-terminated edges of the basic structural units or other species of hydrogen may have an additional impact on the catalyst preparation and also the catalyst performance (15).

Recently, the interdependence of certain surface oxides, the effects of hydrogen spillover, and the hydrogasification of reactive unsaturated carbon atoms on activated carbons containing platinum has been demonstrated (17). Furthermore, for the case of Pd/C-catalysts, the H absorption and desorption kinetics and the H-sorption capacity of the finely dispersed precious metal itself may also be of catalytic relevance.

---

[1] Corresponding author. E-mail: Dr_Peter.Albers@degussa.de.

0021-9517/99 $30.00

The inelastic neutron scattering (INS) technique is ideally suited to observe protons in finely dispersed materials such as carbon blacks or coals (18–21). The penetration depth of neutrons in carbonaceous materials is such that the bulk is probed. This contrasts to X-ray photo-electron spectroscopy (XPS) or SIMS or techniques such as infrared and Raman spectroscopies which probe essentially the surface or near-surface regions of the particles. Because the cross section for protons is more than one order of magnitude greater than for any other atom, hydrogenated entities can be observed even at concentrations much lower than 1 wt%, as usually encountered in carbon blacks. The scattering cross section of C atoms is so weak that in most cases the carbonaceous matrix is not observed directly. However, INS spectra may reveal changes in the hydrogen-containing structures presumably involved in interactions between the metal and its support and on the degree of disorder of the carbon structure (21, 22). In this paper we present the results of physical and chemical characterisation of supported Pd-catalysts. The influence of the HCl-treatment of the carbon supports on catalytic performances is emphasized. INS spectra of some of the supports and catalysts are analyzed. The observed proton dynamics reveal some consequences of the various processes such as acid treatment, reduction, palladization, and hydrogen-loading onto the hydrogen-containing entities in activated carbon, carbon blacks, and the supported Pd-particles.

## EXPERIMENTAL

### *Catalyst Preparation*

The support materials used for the preparation of the Pd-catalysts are specified in Table 1. The carbons were steam activated. The total porosity of the pelletized and of the powdered activated carbons are rather similar. X-ray fluorescence analysis (XRF) and SIMS measurements showed similar impurity levels for surface and bulk. Trace contamination by S, Si, and Cl were observed for the carbon blacks, and traces of Ca, Mg, Na, Al, N, Cl, P, and Si for the activated carbons. The impact of a pronounced surface enrichment of (e.g.) Fe on the catalysts preparation and performance (14) was therefore ruled out. Transmission electron microscopy (TEM) reveals significant differences in the microstructure (crystallinity and degree of graphitization) of the supports (Fig. 1).

**TABLE 1**

**Support Materials Used for the Preparation of the Pd Catalysts**

| Support material/origin | Nitrogen surface area $m^2/g$ | Bulk density g/l | Hydrogen content[a] (wt%) | Ash content (wt%) |
|---|---|---|---|---|
| Activated carbon powder/ pine wood | ≈1150 | 180 | 1.1 | 3.5 |
| Activated carbon pellets/ beech wood | ≈1300 | 380 | 0.9 | 8 |
| Carbon black/ furnace black | 234 | 280 | 0.38 | <0.2 |
| Graphitized carbon black/ furnace black | 72 | 310 | 0.03 | <0.2 |

[a] Determined by CHN-analysis.

The carbon supports were loaded with Pd either in their original state or after HCl-treatment performed with a 2 *M* HCl solution, according to a standard procedure (15). This treatment predominantly removed the ash and the inorganic impurities whilst the total porosity remained largely unchanged. The ash content of the starting materials (Table 1) was lowered to a level of <1 wt% for the pelletized activated carbon support, to <0.5 wt% for the powdered activated carbon and to <0.1 wt% for the carbon blacks. Monitoring the trace contaminations of activated carbons by means of XRF and SIMS showed that, in particular, the contents of Ca, Mg, Na, and Si were lowered by HCl-treatment. Regarding the carbon blacks only the levels of Si and Cl were reduced, whereas the amount of S remained largely constant. X-Ray photo-electron spectrometry (XPS) showed binding energy values of the S 2p signal at 163.7–164.1 eV indicating the presence of predominantly sulfane-like sulfur species which are bonded to the basic structural units, whereas species such as sulfates or sulfonates or of sulfidic S were mostly missing.

HCl was chosen to focus the study on the effects of a generally nonoxidative modification procedure on the properties of catalytic relevance.

All catalysts were prepared using $H_2PdCl_4$ at a constant Pd-loading of 5 wt%. The powdered catalysts prepared on graphitized carbon black, carbon black, or activated carbon derived from pine wood were reduced using a wet chemical process (15). The support material was first suspended in distilled water. Then an aqueous solution of the Pd-compound was added. After impregnation and heating to 80°C the suspension was adjusted to pH 10 by adding NaOH. After agitation the precious metal was reduced by adding formaldehyde. After further agitation the suspension was filtered and washed with distilled water. The pelletized catalysts were prepared by adding tetrachloropalladeous acid to the activated carbon pellets in a shaker. The volume of the solution containing precious metal was calculated to be 95% of the total adsorption capacity of the activated carbon pellets, according to the determined pore volume. After impregnation, the pellets were dried and reduced in a flowing gaseous mixture: $N_2/H_2$ (95/5).

The catalytic activities of the materials were determined in a standard test reaction by hydrogenating cinnamic acid

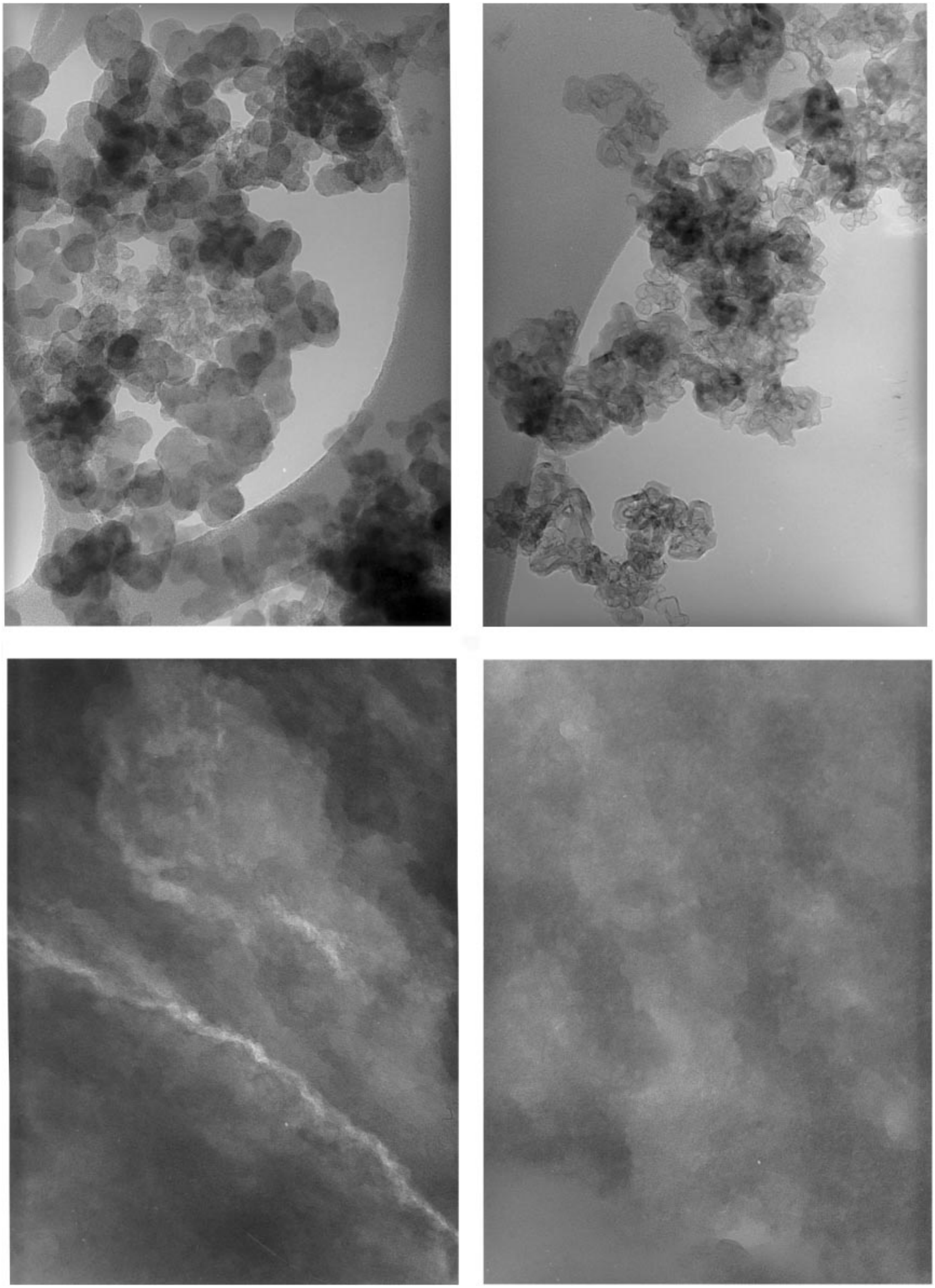

**FIG. 1.** Transmission electron micrographs of the different support materials: upper left, carbon black (on porous carbon foil); upper right, graphitized carbon black (on porous carbon foil); lower left, activated carbon derived from beech wood (thin section cut from a pellet); lower right, activated carbon derived from pine wood (thin section cut from a particle). E-magnification: 100000x.

**TABLE 2**

**Characterization of the 5 wt% Pd/C-Catalysts**

| Support material pretreatment | CO-chemisorption (ml CO/g catalyst) | Precious metal dispersion[a] (%) | Catalytic activity[b] (ml $H_2$/min · g) | Pd-surface concentration[c] |
|---|---|---|---|---|
| Graphitized carbon black/original | 0.98 | 9.3 | 169 | 0.91 |
| Graphitized carbon black/HCl | 1.06 | 10.1 | 262 | 1.65 |
| Carbon black/original | 1.82 | 15.4 | 297 | 0.53 |
| Carbon black/HCl | 1.91 | 18.1 | 479 | 0.56 |
| Activated carbon pellets/original | 1.07 | 10.5 | n.d. | 5.32 |
| Activated carbon pellets/HCl | 1.26 | 11.9 | n.d | 6.56 |
| Activated carbon powder/original | 1.43 | 13.6 | 715 | 7.58 |
| Activated carbon powder/HCl | 2.32 | 22.1 | 926 | 8.97 |

[a] Calculated from CO-chemisorption data.

[b] Determined by hydrogenation of cinnamic acid (not applicable for the pelletized support).

[c] In percentage of area, as determined by means of XPS.

(Degussa standard operation procedure A101) and are compiled in Table 2. Two hundred milligrams of catalyst were suspended in a cinnamic acid/ethanol mixture in a hydrogenation reactor. The hydrogen consumption was monitored for a time of 8 min at 25°C at a stirring velocity of 2000 rpm.

TEM gives an average size for the palladium particles of ~2.5 nm on the powdered activated carbon prepared from pine wood, ~3.5 nm on the carbon black, and ~5 nm on the graphitized carbon black. With the pelletized support derived from beech wood, a shell-type catalyst was obtained. Apart from coarse Pd crystallites on the outer perimeter of the pellets, the average particle size of the finely divided fraction of the Pd was ~4.5 nm.

According to XPS measurements, the surfaces of the finely divided Pd-particles were partially covered with a thin layer of chemisorbed oxygen. This could be removed rapidly by short-time bombardment with $Ar^+$ ions or by *in-situ* reduction with hydrogen in an environmental cell attached to the spectrometer.

Previous investigations have shown that the analysis of the INS spectra of activated carbon can be hampered by excessive amounts of adsorbed $H_2O$ molecules; see Fig. 2A in Ref. (21). Therefore, both the raw materials and the final catalysts were first carefully dried *in vacuo* at 105°C and then stored in a vacuum desiccator over granular phosphorous pentoxide. The drying procedures were performed under constant conditions. They were monitored using gravimetric methods.

Hydrogen-loading (purity 99.999%, Messer–Griesheim) of the catalysts was performed directly in thin-walled Al containers. The H-sorption equilibrium was established within seconds for the palladized carbon blacks. It took a slightly longer time for the Pd-catalysts on activated carbon with high porosity. The observed hydrogen-sorption isotherms deviate from the ideal shape of the $\alpha$-/$\beta$-plateau region usually observed for bulk Pd or Pd-black (23, 24). This may be attributed to a disturbance of long-range coherence in the small supported Pd particles. Long-range stress effects are believed to be responsible for the $\alpha$-/$\beta$-phase transition and the corresponding flat plateau region in the phase diagrams of bulk palladium or palladium black (23–26).

### *INS Spectra*

INS spectra were measured with the TFXA-spectrometer (time focused crystal analyzer) at the spallation neutron source ISIS (Rutherford Appleton Laboratory, UK). The spectrometer exploits geometric time focusing and software energy focusing so as to give a rather flat energy dependence of the resolution of ~3% in $\Delta E/E$. The beam size was about 2 cm × 5 cm so that a representative macroscopic amount of a sample could be monitored.

Carbon samples (6–11 g) were wrapped in thin aluminium foil and loaded into a closed-cycle refrigerator at 30 K. About 10–15 g of the Pd-catalysts in sealed aluminium containers were slowly cycled (i.e., conditioned by H-loading and deloading) four times with hydrogen at room temperature in order to remove the thin layer of chemisorbed oxygen from the finely dispersed palladium particles. This treatment is known to optimize the hydrogen sorption properties of the Pd as well.

Prior to the final hydrogenation step, the catalyst was pumped down to $10^{-3}$ mbar and was finally hydrogenated up to sorption equilibrium at 500 or 800 mbar, respectively (*v.i.*). It was observed that the final hydrogen-sorption capacity of the catalysts obtained with HCl-treated carbons was slightly enhanced by these processes.

The data acquisition time was about 8 h for each sample, this being a compromise between statistics and beam time available. The rather voluminous samples were prequenched with liquid nitrogen to reduce the cooling time in the cryostat of the TFXA spectrometer. Unfortunately, the quenching procedure resulted in nitrogen being trapped and frozen in some of the samples wrapped in the Al sachets. This resulted in the appearance of an intense peak centred at $\sim$50 $\text{cm}^{-1}$, with maxima at 36 and 47 $\text{cm}^{-1}$ which was apparent in some of the spectra. At higher frequencies, the only other feature caused by solid nitrogen is the very weak $N\equiv N$ stretch which is moved from its gas-phase recoil-shifted value (27) of 2360 $\text{cm}^{-1}$ to 2500 $\text{cm}^{-1}$. Thus, in the spectral region of interest in the INS spectra (100–2000 $\text{cm}^{-1}$), the presence of solid nitrogen does not affect the conclusions of the work.

The weak background spectrum of the empty aluminium can was subtracted.

The neutron-scattering cross sections of the samples were such that less than about 10% of the incident neutrons were scattered. Multiple-scattering events are thus negligible. Spectra were normalized with respect to the amount of sample in the beam.

## RESULTS AND DISCUSSION

### Catalyst Characterisation

The palladium catalysts were characterized with different techniques (Table 2). Results for the CO chemisorption, precious metal dispersion, and catalytic activity for the hydrogenation of cinnamic acid increase significantly with the acid treatment of the support. The effect is most pronounced for the powdered activated carbon support. A significant improvement of the catalytic acitivity was also observed for the hydrogenation reactions with the fixed-bed catalyst pellets.

It is remarkable that acid treatments enhance the catalytic efficiencies for both the low surface area, nearly nonporous, and very pure graphitized carbon black support and the large surface area, highly porous, and ash-containing activated carbon powders (Table 1). This suggests some principal similarities between properties at the surfaces of the carbon blacks and the activated carbon supports being of relevance in the catalyst preparation.

Figure 2 shows TEM images of the final Pd catalysts. The contribution of coarse Pd particles found with the activated

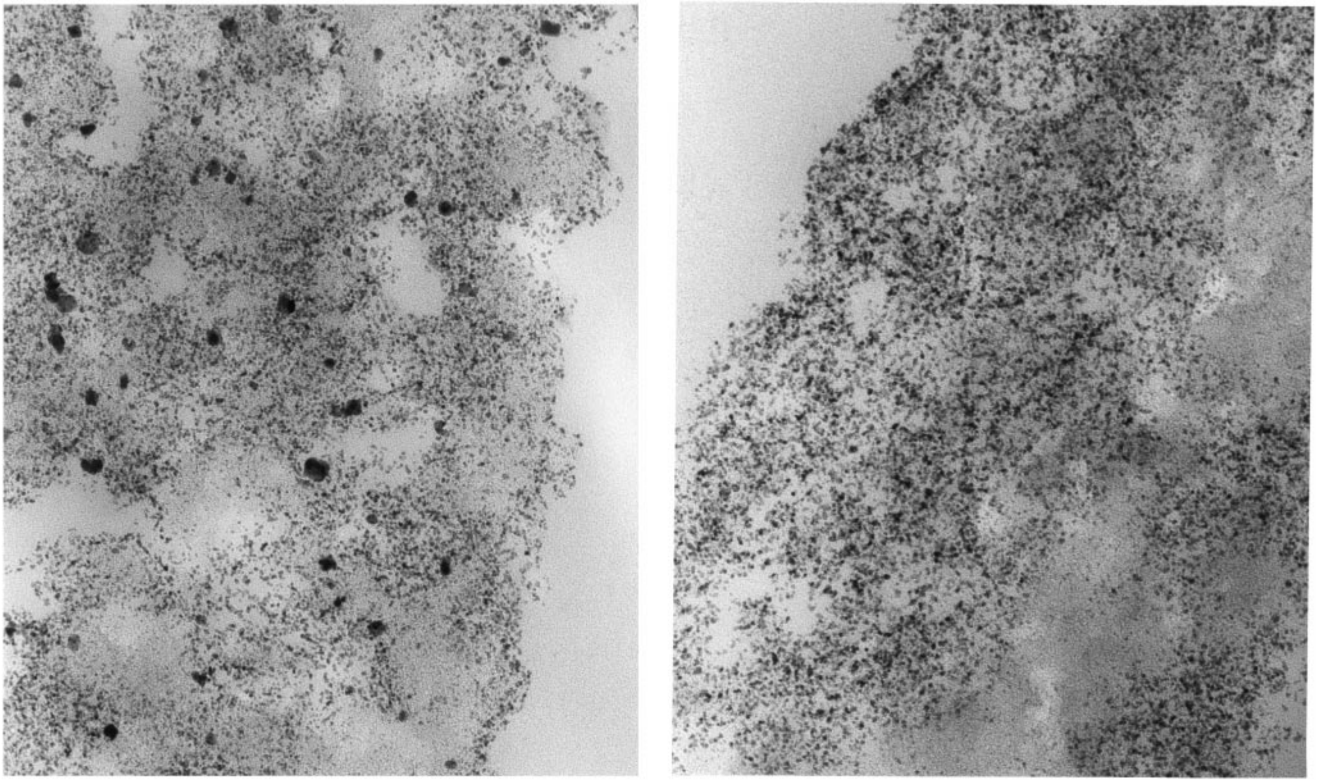

**FIG. 2.** Pd particles on activated carbon derived from pine wood (thin section cut from a particle): left, prepared on the original support; right, prepared on the HCl-treated support. E-magnification: 100000X (see Table 3).

**TABLE 3**

**On the Influence of the Acid Treatment on the Precious Metal Particle Size Distribution as Determined by Statistical Evaluation of TEM Data on Graphitized Carbon Black and on Activated Carbon (Powder) Derived from Pine Wood**

| 5% Pd/C Support | Original | | | HCl-treated | | |
|---|---|---|---|---|---|---|
| | DN (nm) | DA (nm) | OEM ($m^2/g$) | DN (nm) | DA (nm) | OEM ($m^2/g$) |
| Graph. black | 5,0 | 7,2 | 68,9 | 5,1 | 5,8 | 86,6 |
| Activ. carbon | 2,6 | 4,6 | 108,1 | 2,5 | 2,6 | 188,6 |

*Note.* $DN = (\sum n_i d_i)/N$, particle size, arithmetical average. $DA = (\sum n_i d_i^3)/(\sum n_i d_i^2)$, particle size, averaged over the surface. ($DN = DA \rightarrow$ monodisperse system.) $OEM = 6000/(DA \bullet \rho)$ $m^2/g$, specific TEM-precious metal surface area.

pine wood support in its original condition are absent for the HCl treated and cleaned support material. The same effect was observed for Pd on carbon blacks. It appears that the acid treatment of the support narrows the distribution function for the Pd particle size, specifically at the surface of the support (see Table 3). This narrowing seems to be correlated with an increase of the catalytic activity. The observation may suggest that the acid treatment was suitable to lower efficiently the relative amounts of critical adsorption sites or impurity centres which in the original condition of the support may act as sites for particle growth.

XPS confirms changes of the Pd concentrations and dispersion at the surface after acid treatment (Table 2).

## INS Spectra

### *Activated Carbon and Pd-Activated Carbon Catalysts*

Figures 3–7 show the INS spectra obtained. Most of the INS intensity is due to protons associated to the carbon matrix. The INS spectra of all samples give rather broad bands, as anticipated for such disordered materials. These bands are superimposed on a continuum with almost constant intensity over the whole spectral range. On the basis of previous work on coals and carbon blacks (18–22), the continuum of intensity is attributed to the recoil of particles with mass 1 amu. These particles are not chemically bound to any atom. Therefore, they behave as a gas of free particles. However, INS provides no information on the effective charges for these particles. With this technique, it is not possible to distinguish $H^+$, $H^0$, $H^-$, or entities with intermediate charge. In line with previous work (18–20, 28), these entities are referred to as free recoiling protons, since neutrons are scattered by nuclei. The continuum intensity is not related to the amount of free particles in a simple way (28).

Broad bands superimposed on this continuum correspond to vibrations of protons bound to heavy atoms (C, O, S). The broad bands at 900 and 1200 $cm^{-1}$ correspond to aromatic CH-bending modes. The dip of intensity at 1000 $cm^{-1}$ is specific to rather large polyaromatic species with graphite-like structure. The C-H bending modes in nonconjugated structures are anticipated at 1300–1500 $cm^{-1}$. H-stretching modes appear with only weak intensities around 2900–3100 $cm^{-1}$. It can be concluded that the INS-spectra of the activated carbons investigated are closer to carbon blacks (21, 22) than to coals (18–20). A more or less sharp or well-resolved band was measured at ~100 $cm^{-1}$, due to lattice modes of the graphite-like structure (29) which also confirms the enhanced aromaticity/graphiticity of this material.

After Pd impregnation and reduction (Fig. 3B) weak features at about 830 and 920 $cm^{-1}$ may tentatively be attributed to H vibrations at the surface of the Pd particles (30, 31). After the hydrogenation treatment of the Pd catalyst obtained on the original support without HCl purification two new bands appear at about 450 and 610 $cm^{-1}$ superimposed on the broad spectrum of the carbon support (Fig. 3C) in the energy range where the localized modes of protons at octahedral sites in the $\alpha$- and the $\beta$-phase of bulk, finely divided or supported Pd are anticipated (32–38). Compared to a study on the hydride formation of 1.5 nm Pd particles in Y-zeolite (39), the rather high hydrogen content of the activated carbon support ($H_c$) (Table 1) gives quite unfavourable conditions for the detection of the vibrational contributions of protons dissolved in the Pd particles ($H_{Pd}$). The $H_c/H_{Pd}$-ratio for the hydrogenated catalyst is about 18. Nevertheless, the INS bands of the Pd hydrides are rather sharp and narrow (32–38), compared to the rather broad C-H vibrational bands of the activated carbon support which, together with the background due to free recoil protons, extend over a broad spectral range. For the given sample weight and geometry about $3.5 \times 10^{21}$ Pd atoms with roughly the equivalent number of protons were in the beam. This number of protons is well within the hydrogen detection range of the TFXA spectrometer. Therefore, in the following these bands will be attributed to features due to supported palladium hydride.

After dehydrogenation of the catalyst (5 min at 60°C under vacuum, Fig. 3D), the bands at 450 and 610 $cm^{-1}$ disappeared, suggesting the decomposition of the hydride phases of Pd, as expected.

Therefore, these bands were only observed on the hydrogenated catalyst measured under a sorption equilibrium pressure of 800 mbar $H_2$ (Fig. 3C). They were missing on the original carbon sample, as well as on the original Pd catalyst before hydrogenation and after dehydrogenation (Figs. 3A, B, D). These observations may support the interpretation that the bands at 450 and 610 $cm^{-1}$ were due to Pd-hydride.

Comparision of the spectra 3A and 3D shows differences, possibly due to the removal of some lower crystalline carbon species during the catalyst preparation and the hydrogenation/dehydrogenation cycles. Lower crystalline and disordered carbonaceous species were observed to show broad vibrational features below 800 $cm^{-1}$ extending down to 500 $cm^{-1}$ (21, 22).

After HCl-treatment, the activated carbon (Fig. 4A) gives a spectrum significantly different from the untreated carbon (Fig. 3A). The fine features in the range below 800 $cm^{-1}$ to 400 $cm^{-1}$ show small differences, possibly due to the removal of ash contributions and the eluation of adsorbed species, while the remaining peaks at 454, 522,

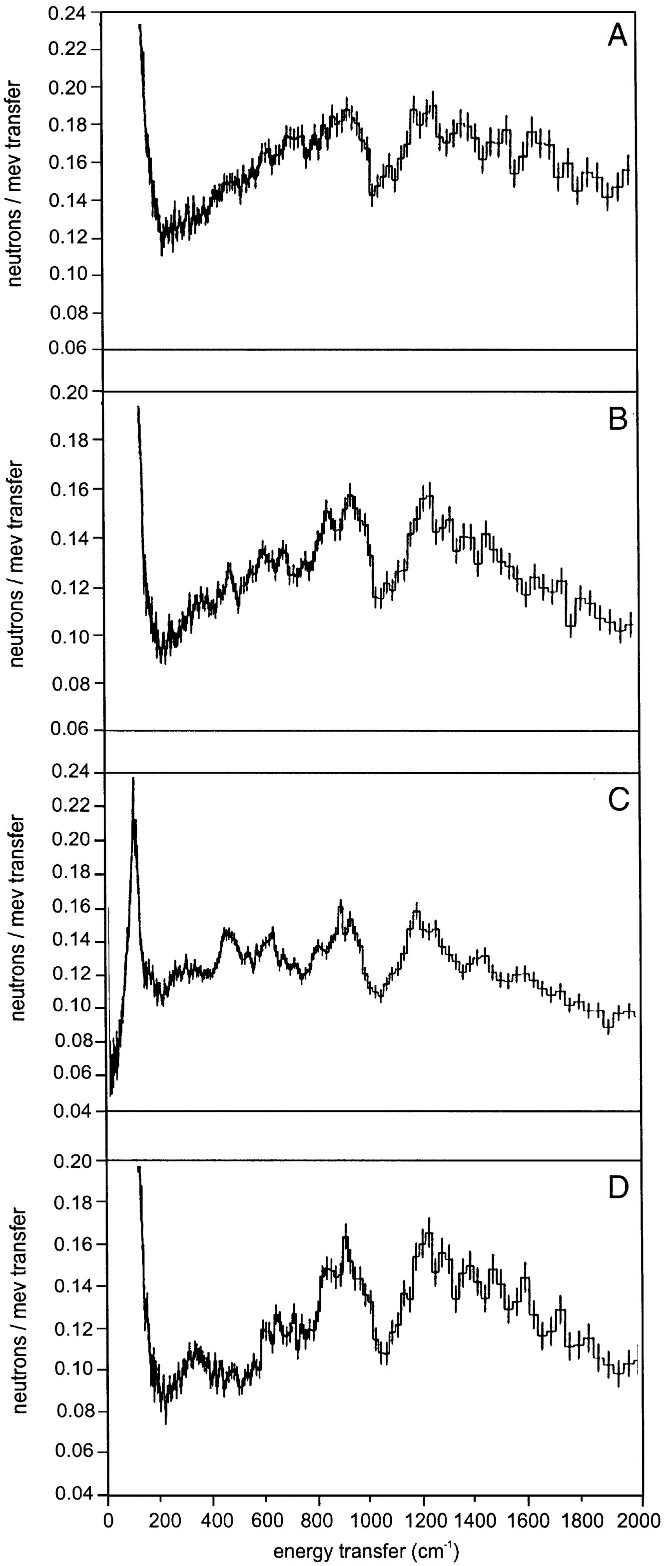

**FIG. 3.** INS spectra of steam activated carbon derived from beech wood and of the corresponding Pd/C-catalysts: A, original, dried; B, original, loaded with 5 wt% Pd, dried, reduced with $H_2/N_2$ (5/95); C, as B, after hydrogen treatment *in-situ*, measured under 800 mbar of hydrogen; D, as C, after hydrogen removal under vacuum conditions (5 min at 60°C, turbomolecular pump).

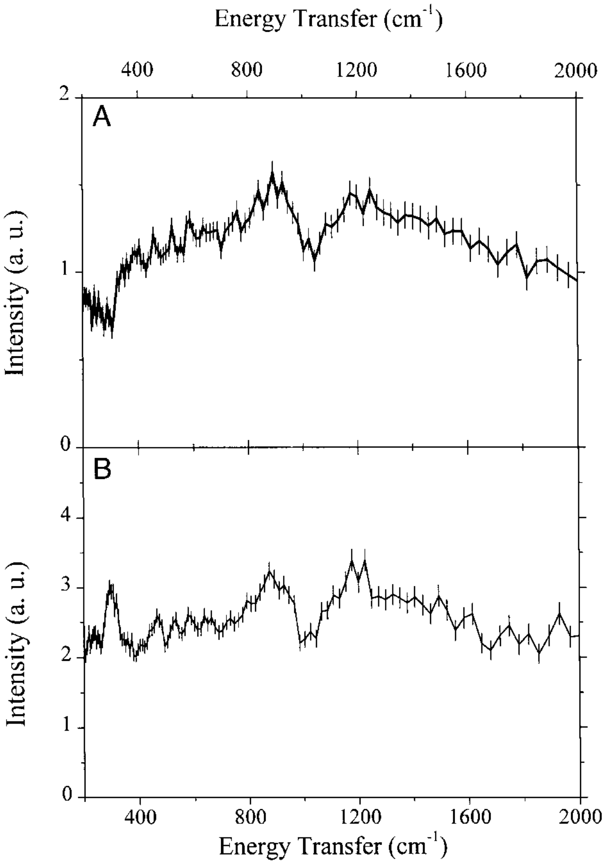

**FIG. 4.** INS spectra of steam-activated carbon, derived from beech wood and on the corresponding Pd/C-catalyst: A, original, after HCl-treatment of the support; B, HCl-treated support, loaded with 5 wt% Pd, dried, reduced with $H_2/N_2$, after hydrogen treatment *in-situ*, measured under 500 mbar of hydrogen.

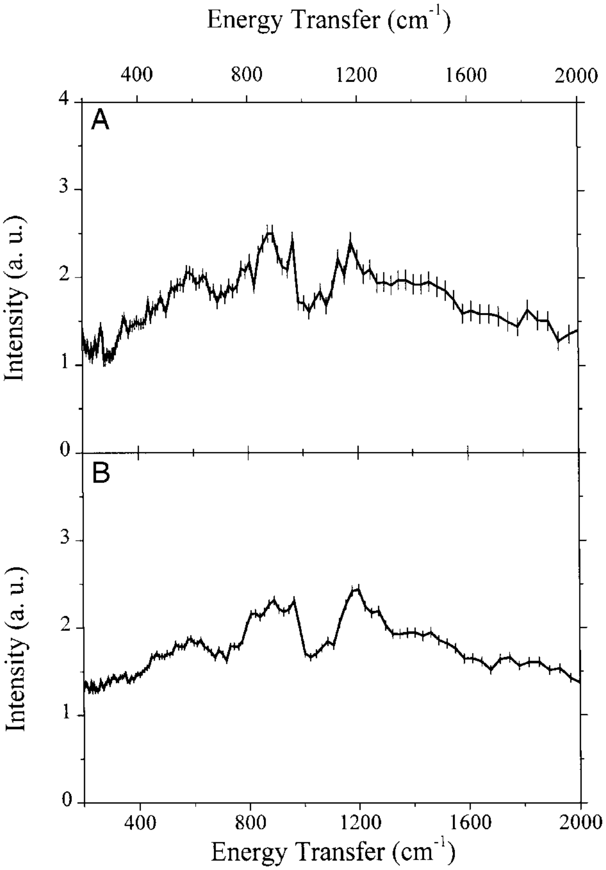

**FIG. 5.** INS spectra of steam-activated carbon derived from pine wood: A, original support, dried; B, HCl-treated support, dried.

and 588 cm$^{-1}$ indicate the presence of chemically bound polyaromatic species which were not removed by the acid treatment.

Comparing the spectra of the HCl-treated support after palladization, reduction, and hydrogen loading (Fig. 4B) with the corresponding spectrum of the Pd catalyst (Fig. 3C) on the untreated carbon support and with the other support materials shows a more pronounced intensity of a band at 301 cm$^{-1}$ and of additional weak features at about 467, 527, 581, 651 cm$^{-1}$ in Fig. 4B. In contrast to Fig. 3C it is hard to identify any contributions due to Pd-hydride expected in the range 464–480 cm$^{-1}$ or 532–590 cm$^{-1}$ from these rather similar and narrow vibrational features. These narrow signals resemble the shape and energy range of molecular structures obtained as products of a hydrogasification treatment on the surface of carbon black (22) or the signals measured for polyaromatic molecules or polynuclear aromatic hydrocarbon structures derived from heat-treated naphthalenes (40).

Indications of these vibrational features could already be roughly resolved on the HCl-purified support (Fig. 4A) but the relative signal intensity, especially at about 301 cm$^{-1}$, is strongly enhanced. This illustrates that significant changes occurred in the material during the course of acid purification, palladization, and hydrogenation.

Considerably lower changes due to acid treatment were observed for the activated carbon powder (derived from pine wood), before and after HCl-treatment (Fig. 5A and B), which contains a significantly lower amount of ashes (Table 1).

### *Comparision of Hydrogasification Effects on Pd-Activated Carbon and Carbon Black*

The detail spectra in Fig. 6 show that the vibrational features observed on the Pd/C-sample (Fig. 4B) show significantly higher energy values than are observed for the related molecular species which were obtained by a noncatalytic hydrogasification treatment of a carbon black (350 bar $H_2$, 350°C) appearing at 230, 350, 470, and 530 cm$^{-1}$ (22). Extraction experiments gave evidence that the molecular species which were indicated by these narrow vibrational bands were still chemically bonded to the carbon black surface.

With increasing molecular mass and increasing degree of polycondensation/annelation the INS vibrational features of polyaromatic molecules show shifts to lower energy. This follows from comparing the INS-spectra of perylene (19), anthracene, phenanthrene, acenaphthene (41). It

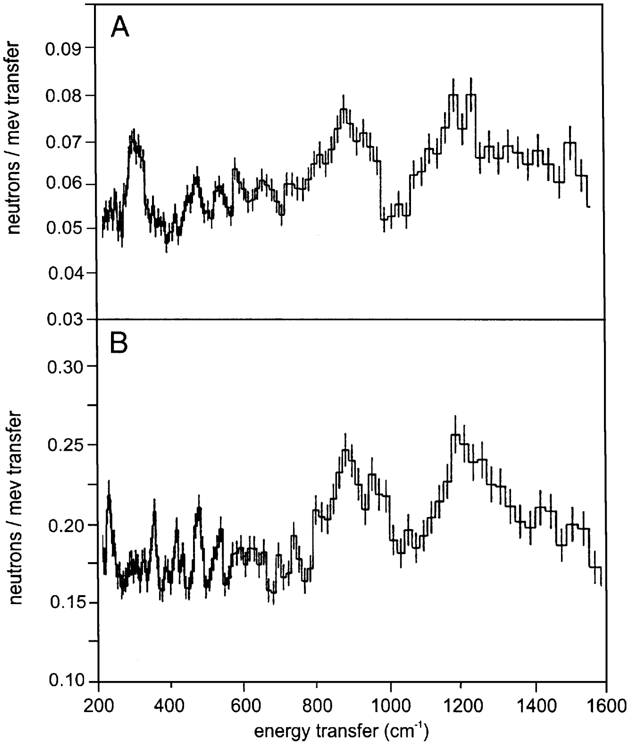

**FIG. 6.** Comparision of the low energy region of the INS spectra of: A, Pd/activated carbon catalyst as measured under 500 mbar hydrogen loading (detail from Fig. 4B); B, furnace black after noncatalytic hydrogasification treatment (detail region of a spectrum from (22)).

follows that the average size of the molecular-like species obtained at the surface of carbon black by a noncatalytic high-temperature hydrogasification was significantly larger than on the hydrogenated palladized activated carbon (Figs. 4B and 6A) which was previously purified by HCl-treatment. Considering the results of Menedez *et al.* (17) on the hydrogasification of reactive unsaturated carbon structures on platinized activated carbons due to spillover of atomic hydrogen it appears that the surface of the HCl-treated support shows an especially enhanced sensitivity to the attack of activated hydrogen during the hydrogenation of the Pd-catalyst *in situ*. Changes in the relative amounts of adsorbed water molecules (see Fig. 2A in Ref. (21)) and especially the lowering of the ash content of the carbon support due to the HCl-treatment may contribute to the enhanced amounts and accessability of active and reactive sites, being of relevance for the adsorption of Pd atoms as well as for the spillover of active hydrogen species.

Further investigations are necessary to clarify in more detail as to whether or not the different results of catalytic and noncatalytic hydrogasification reactions as shown in Fig. 6 can be explained exclusively by slower kinetics of the noncatalytic process and as to how the results are affected by increasing the time of hydrogenation.

The partial hydrogasification of the carbon surface by spillover of atomic or active hydrogen from the Pd-particles may compete with the formation of Pd-hydride. This would explain why indications of the vibrational bands of palladium hydride were observed on the original activated carbon support (Fig. 3C) but were largely missing on the HCl treated activated carbon (Fig. 4B).

The enhancement of the relative amounts of polyaromatic entities on the catalyst surface corresponds to enhanced disorder on the molecular scale. Polyaromatic entities attached to the carbon surface presumably might be addressed as active sites which could also be of some relevance for the adsorption of reactants in the catalytic applications.

### *Pd on Carbon Black*

In the case of the ungraphitized carbon black support, the relative intensity of the sharp features at 460 and 620 $\mathrm{cm}^{-1}$ were scarcely differentiated from the broad bands of the C-H bending modes and from the band around 500 $\mathrm{cm}^{-1}$ due to residual amounts of disordered carbon in the support. For the graphitized carbon black, the effects of Pd-loading, followed by hydrogenation (Fig. 7B) are similar to those observed for the palladized sample in Fig. 3C. There is a strong peak due to $\beta$-palladium hydride at 453 $\mathrm{cm}^{-1}$ and a weak feature from $\alpha$-Pd hydride at about 620 $\mathrm{cm}^{-1}$. The Pd-hydride peaks appear to be rather sharp and strong because the hydrogen contribution from the graphitized support material, being a nearly nonhydrogenous support, is very small compared to the activated carbon spectra in Fig. 3. Considering the hydrogen content of the graphitic carbon support $H_c$ (Table 1) for the fully loaded $\beta$-Pd-phase a $H_c/H_{Pd}$-ratio of 0.6 is obtained which is much more favourable for the detection of the hydrogen vibrations of the supported Pd-hydride particles than is the case of activated carbon (Fig. 3C).

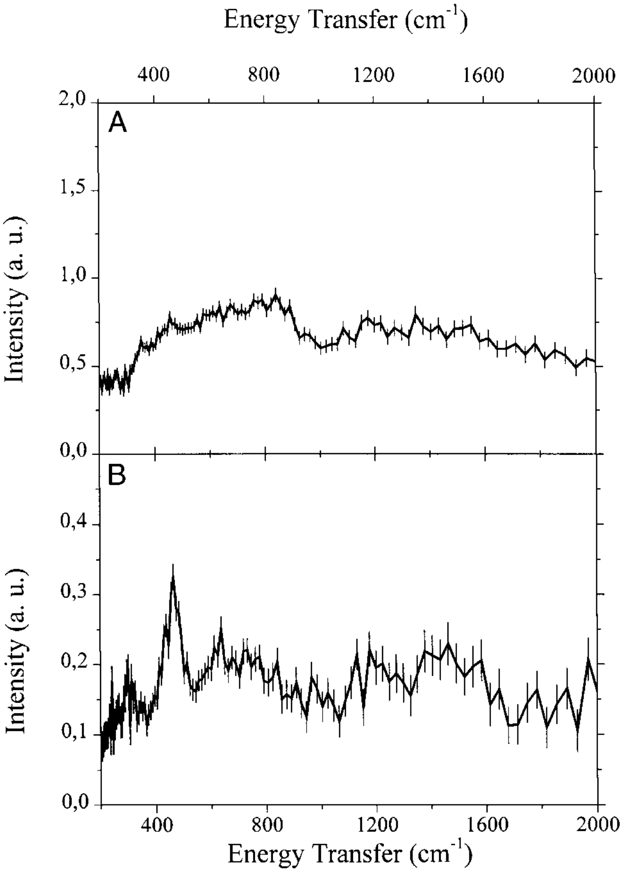

**FIG. 7.** INS spectra of Pd/carbon black catalysts under hydrogen loading. Carbon blacks impregnated with 5 wt% Pd, dried, reduced with $H_2/N_2$ (5/95), after hydrogen treatment *in-situ*: A, Pd/furnace black, 500 mbar $H_2$; B, Pd/graphitized furnace black, 800 mbar $H_2$.

Finally, in agreement with the reported behaviour of carbon blacks (21), the neutron spectra did not give any evidence for the presence of molecular hydrogen (42) in the carbons observed.

## CONCLUSIONS

HCl treatments of graphitized carbon black, carbon black, and activated carbons derived from pine wood or beech wood have positive effects on the efficiency of palladium catalysts. The precious metal dispersion is enhanced, the particle-size distribution is narrowed, the concentration of Pd particles at the surface is increased, and the hydrogenation activity of the final catalysts is improved. This was, surprisingly, observed for activated carbons as well as for carbon black and graphitized carbon black.

Pd catalysts on activated carbon derived from beech wood in both the original and the acid-treated condition showed indications of different sensitivities of the surfaces to hydrogasification effects. Indications of the formation or enhancement of new molecular-like polyaromatic structures were obtained especially on HCl-treated activated carbon. An increasing concentration of these new molecular sites at the carbon surface is an additional positive influence on the precious metal dispersion in the final catalyst and on the adsorption properties of the material.

The observed spectra suggest that the average size of these molecular-like structures is lower than in the case of a noncatalytic hydrogasification treatment of carbon surfaces. The generation of these new sites is promoted by the removal of ash and of adsorbed species during purification of the support by acid treatment and by the enhanced spillover of activated hydrogen from palladium particles to the adjacent surface sites.

Enhanced spillover of activated hydrogen or atomic hydrogen species from Pd to reactive sites on the support may partly compete with the formation of palladium hydride.

## ACKNOWLEDGMENTS

The Rutherford Appleton Laboratory (UK) is thanked for access to neutron beam facilities. F. Fillaux (LASIR, CNRS, France) is gratefully acknowledged for information on unpublished data and for many helpful discussions. K. Simon (Degussa AG) is thanked for the skillful preparation of the catalysts.

## REFERENCES

1. Boehm, H. P., and Knözinger, H., *in* "Catalysis—Science and Technology" (J. R. Anderson and M. Boudart, Eds.), Vol. 4, p. 39. Springer-Verlag, Berlin, 1983.
2. von Kienle, H., and Bäder, E., "Aktivkohle und ihre industrielle Anwendung," p. 52. Enke, Stuttgart, 1980.
3. Radovic, L. R., and Rodriguez-Reinoso, F., Carbon materials in catalysis, *in* "Chem. Phys. Carbon" (P. Thrower, Ed.), Vol. 25, p. 243. Dekker, New York, 1997.
4. Burmeister, R., Despeyroux, B. M., Deller, K., Seibold, K., and Albers, P., "Stud. Surf. Sci. Catal." (M. Guisnet, J. Barbier, J. Barrault, C. Bouchoule, D. Duprez, G. Perot, and C. Montaissier, Eds.), Vol. 78, p. 191. Elsevier, Amsterdam, 1993. [U.S. Patent 5,449,655]
5. Donnet, J. B., *Carbon* **20**, 266 (1982).
6. Ehrburger, P., *Carbon* **29**, 763 (1991).
7. Fu, R., Zeng, H., Lu, Y., Lai, S. Y., Chan, W. H., and Ng, C. F., *Carbon* **33**, 657 (1995).
8. Richard, R., and Gallezot, P., *in* "Preparation of Catalysts IV" (B. Delmon, P. Grange, P. A. Jacobs, and G. Poncelet, Eds.), p. 71. Elsevier, Amsterdam, 1987.
9. van Dam, H. E., and van Bekkum, H., *J. Catal.* **131**, 335 (1991).
10. Rodriguez-Reinoso, F., Molina-Sabio, M., and Munecas, M. A., *J. Phys. Chem.* **96**, 2707 (1992).
11. Roman-Martinez, M. C., Cazorla-Amoros, D., Linares-Solano, A., Salinas-Martinez de Lecea, C., Yamashita, H., and Anpo, M., *Carbon* **33**, 3 (1995).
12. Prado-Burguette, C., Linares-Solano, A., Rodriguez-Reinoso, F., and Salinas-Martinez de Lecea, C., *J.Catal.* **115**, 98 (1989).
13. Daly, F. P., Jensen, W. M., and Ostgard, D. J., *in* "Catalysis of Organic Reactions" (N. G. Scaros and M. L. Prumer, Eds.), p. 13. Dekker, New York, 1995.
14. Albers, P., Deller, K., Despeyroux, B. M., Schäfer, A., and Seibold, K., *J. Catal.* **133**, 467 (1992).
15. Albers, P., Deller, K., Despeyroux, B. M., Prescher, G., Schäfer, A., and Seibold, K., *J.Catal.* **150**, 368 (1994).
16. Albers, P., Freund, B., Prescher, G., Seibold, K., and Wolff, S., *KGK Kautschuk Gummi Kunststoffe* **48**, 336 (1995). [English]
17. Menendez, J. A., Radovic, L. R., Xia, B., and Phillips, J., *J. Phys. Chem.* **100**, 17243 (1996).
18. Fillaux, F., Papoular, R., Lautie, A., and Tomkinson, J., *Carbon* **32**, 1325 (1994).
19. Fillaux, F., Papoular, R., Lautie, A., and Tomkinson, J., *Fuel* **74**, 865 (1995).
20. Fillaux, F., Papoular, R., Lautie, A., and Tomkinson, J., *J. Noncryst. Sol.* **188**, 161 (1995).
21. Albers, P., Prescher, G., Seibold, K., Ross, D. K., and Fillaux, F., *Carbon* **34**, 903 (1996).
22. Albers, P., Seibold, K., Prescher, G., Freund, B., Parker, S. F., Tomkinson, J., Ross, D. K., and Fillaux, F., Neutron spectroscopic investigations on different grades of modified furnace blacks and gas blacks, *in* "The 23rd Biennial Conference on Carbon, Pennsylvania State University, July 13–18, 1997," Extended Abstracts Vol. II, p. 590. [*Carbon*, accepted]
23. Wicke, E., and Nernst, G. H., *Ber. Bunsenges. Phys. Chem.* **68**, 224 (1964).
24. Frieske, H., and Wicke, E., *Ber. Bunsenges. Phys. Chem.* **77**, 50 (1973).
25. Lewis, F. A., "The Palladium Hydrogen System." Academic Press, London/New York, 1967.
26. Wicke, E., and Brodowsky, H., *in* "Hydrogen in Metals" (G. Alefeld and J. Völkl, Eds.), Vol. 2, Topics in Appl. Phys., Vol. 29, p. 73. Springer, Berlin, 1978.
27. Tomkinson, J., and Kearley, G. J., *J. Chem. Phys.* **91**, 5164 (1989).
28. Fillaux, F., Bennington, S. M., Tomkinson, J., and Yu, L. T., *Chem. Phys.* **209**, 111 (1996).
29. Ross, D. K., *J. Phys. C: Sol. State* **6**, 3525 (1973).
30. Ratajczykowa, I., *Surf. Sci.* **48**, 549 (1975).
31. Howard, J., Waddington, T. C., and Wright, C. J., *Chem. Phys. Lett.* **56**, 258 (1978).
32. Drexel, W., Murani, A., Tocchetti, D., Kley, W., Sosnowska, I., and Ross, D. K., *J. Phys. Chem. Solids* **37**, 1135 (1976).
33. Ross, D. K., Martin, P. F., Oates, W. A., and Khoda-Bakhsh, R., *Z. Phys. Chem. NF* **114**, 221 (1979).
34. Hunt, D. G., and Ross, D. K., *J. Less-Common Met.* **49**, 169 (1976).
35. Nicol, J. M., Rush, J. J., and Kelley, R. D., *Phys. Rev. B* **36**, 9315 (1987). and *Surf. Sci.* **197**, 67 (1988).
36. Rowe, J. M., Rush, J. J., Smith, H. G., Mostoller, M., and Flotow, H. E., *Phys. Rev. Lett.* **33**, 1297 (1974).
37. Braid, I. J., Howard, J., and Tomkinson, J., *J. Chem. Soc., Faraday Trans. 2* **79**, 253 (1983).
38. Jobic, H., Candy, J.-P., Perrichon, V., and Renouprez, A., *J. Chem. Soc. Faraday Trans. 2* **81**, 1955 (1985).
39. Jobic, H., and Renouprez, A., *J. Less-Common Met.* **129**, 311 (1987).
40. Leung, P. S., and Safford, G. J., *Carbon* **8**, 527 (1970).
41. F. Fillaux, unpublished.
42. Honeybone, P. J. R., Newport, R. J., Howells, W. S., Tomkinson, J., Bennington, S. M., and Revell, P. J., *Chem. Phys. Lett.* **180**, 145 (1991).